Electronic Supplementary Material (ESI) for ChemComm.

Supporting Information

Matrix-isolated trifluoromethylthiyl radical: sulfur atom transfer, isomerization and oxidation reactions

Bifeng Zhu,[a] Zhuang Wu,[a] Lina Wang,[a] Bo Lu,[a] Tarek Trabelsi,[b] Joseph S. Francisco,[b,*] and Xiaoqing Zeng[a,*]

[a]Department of Chemistry, Fudan University, Shanghai 200433 (China)
E-mail: xqzeng@fudan.edu.cn
[b]Department of Earth and Environment Science and Department of Chemistry, University of Pennsylvania, Pennsylvania,19104-6243 (USA)
E-mail: frjoseph@sas.upenn.edu

Table of Contents

Experimental and computational details

Sample preparation

Bis(trifluoromethyl)disulfane oxide, $CF_3S(O)SCF_3$, was synthesized by the reaction of $CF_3S(O)Cl$ (95%, Macklin) with $AgSCF_3$ (>95%, TCI). Briefly, commercial trifluomethylsulfinyl chloride (1 mmol, 0.15g) was condensed into a reaction vessel containing silver trifluoromethanethiolate (1.5mmol, 0.31g) and propylene carbonate (1 mL). The mixture was stirred at –50 °C for 72 h. The volatile products were separated by passing through three successive cold U-traps (–64, –86, –196 °C). Pure $CF_3S(O)SCF_3$ was retained in the middle trap. The purity of the substance was checked by gas phase IR (INSA OPTICS FOLI10-R, ν = 1224, 1181, 1112, 763 cm^{-1}) and NMR spectroscopy (Bruker Avance III HD 500 spectrometer). ^{13}C NMR (125 MHz, $CDCl_3$): δ = 124.7 (q, $–S(O)CF_3$), 128.5 (q, $–SCF_3$) ppm. ^{19}F NMR (470 MHz, $CDCl_3$): δ = –33.8 (s, $–S(O)CF_3$), –68.8 (s, $–SCF_3$).

Gases Ar (≥ 99.999%, Linde), N_2 (≥ 99.999%, Linde), Ne (≥ 99.999%, Messer), and O_2 (≥ 99.999%, Linde) were used without further purification. For the isotope labeling experiments, $^{15}N_2$ (98 atom %, Aldrich) and $^{18}O_2$ (97 atom %, Aldrich) were used.

Matrix-isolation IR spectroscopy

Matrix IR spectra were recorded on a FT-IR spectrometer (Bruker 70V) in a reflectance mode using a transfer optic. A KBr beam splitter and MCT detector were used in the mid-IR region (5000–400 cm^{-1}). Typically, 200 scans at a resolution of 0.5 cm^{-1} were co-added for each spectrum. Gaseous $CF_3S(O)SCF_3$ was mixed by Ar, Ne or N_2 (1:1000). As for the oxidation experiment, $CF_3S(O)SCF_3$ was mixed by oxygen and Ar, Ne or N_2 (1:1000) at room temperature. Then the mixture (sample:O_2:dilution gas=1:50:1000, estimated) was passed through an aluminum oxide furnace (o.d 2.0 mm, i.d. 1.0 mm), which can be heated over a length of ca. 25 mm by tantalum wire (o.d. 2.0 mm, resistance 0.4 Ω) and immediately deposited (2 mmol h^{-1}) in a high vacuum (~10^{-6} pa) onto the Au-plated Cu block matrix support (10 K for N_2 and Ar matrix, 3 K for Ne matrix) using a closed-cycle helium cryostat (Sumitomo Heavy Industries, SRDK-408D2-F50H) inside the vacuum chamber. Temperatures at the second stage of the cold head were controlled and monitored using an East Changing TC 290 digital cryogenic temperature controller a Silicon Diode (DT-670). The voltage and current used in the pyrolysis experiments were 5.50 V and 3.12 A, respectively. Photolysis experiments were performed using ArF excimer laser (Gamlaser EX5/250, 3 Hz, 193 nm), Nd^{3+}: YAG laser (266 nm, MPL-F-266, 10 mW), UV lamp (365 nm, 24 W) and blue-light LED (440 nm).

Matrix-isolation UV-vis spectroscopy

Matrix UV-vis spectra were recorded on a Perkin Elmer Lambda 850+ spectrometer (spectral range of 190–800 nm with a scanning speed of 1 nm s^{-1}). The high-vacuum flash pyrolysis products using the similar furnace (o.d 2.0 mm, i.d. 1.0 mm) were deposited onto the CaF_2 matrix support using a closed-cycle helium cryostat (Sumitomo Heavy Industries, SRDK-408D2-F50H) inside the vacuum chamber.

Temperatures at the second stage of the cold head were controlled and monitored using a Lake Shore 335 digital cryogenic temperature controller a Silicon Diode (DT-670). The voltage and current used in the pyrolysis experiments were 5.50 V and 3.12 A, respectively. Photolysis experiments were performed using Ar Fexcimer laser (Gamlaser EX5/250, 3 Hz, 193 nm), Nd^{3+}: YAG laser (266 nm, MPL-F-266, 10 mW), UV lamp (365 nm, 24 W) and blue-light LED (440 nm).

Quantum chemical calculation methods

Structures and IR frequencies of stationary points were calculated using the DFT B3LYP[1], BP86[2] and MPW1PW91[3] methods with the 6-311+G(3df) basis set. Accurate relative energies of the species were further calculated using the complete basis set (CBS-QB3).[4] Local minima were confirmed by vibrational frequency analysis, and transition states were further confirmed by intrinsic reaction coordinate (IRC) calculations.[5] The time-dependent TD-B3LYP/6-311+G(3df)[6] and EOM-CCSD/aug-cc-pV(T+d)Z[7] methods were performed for the prediction of vertical excitations. These computations were performed using the Gaussian 09 software package.[8] To provide detailed insight into the lowest excited states of CF_3S•, •CF_2SF and CF_3SOO•, calculations with the complete active space self-consistent field (CASSCF),[9] followed by the internally contracted multireference configuration interaction including the Davidson correction MRCI+Q[10] were used. These calculations were done using the optimized equilibrium geometries at the CCSD(T)/aug-cc-pv(T+d)z level. All these ab initio calculations were performed with MOLPRO 2019 program.[11]

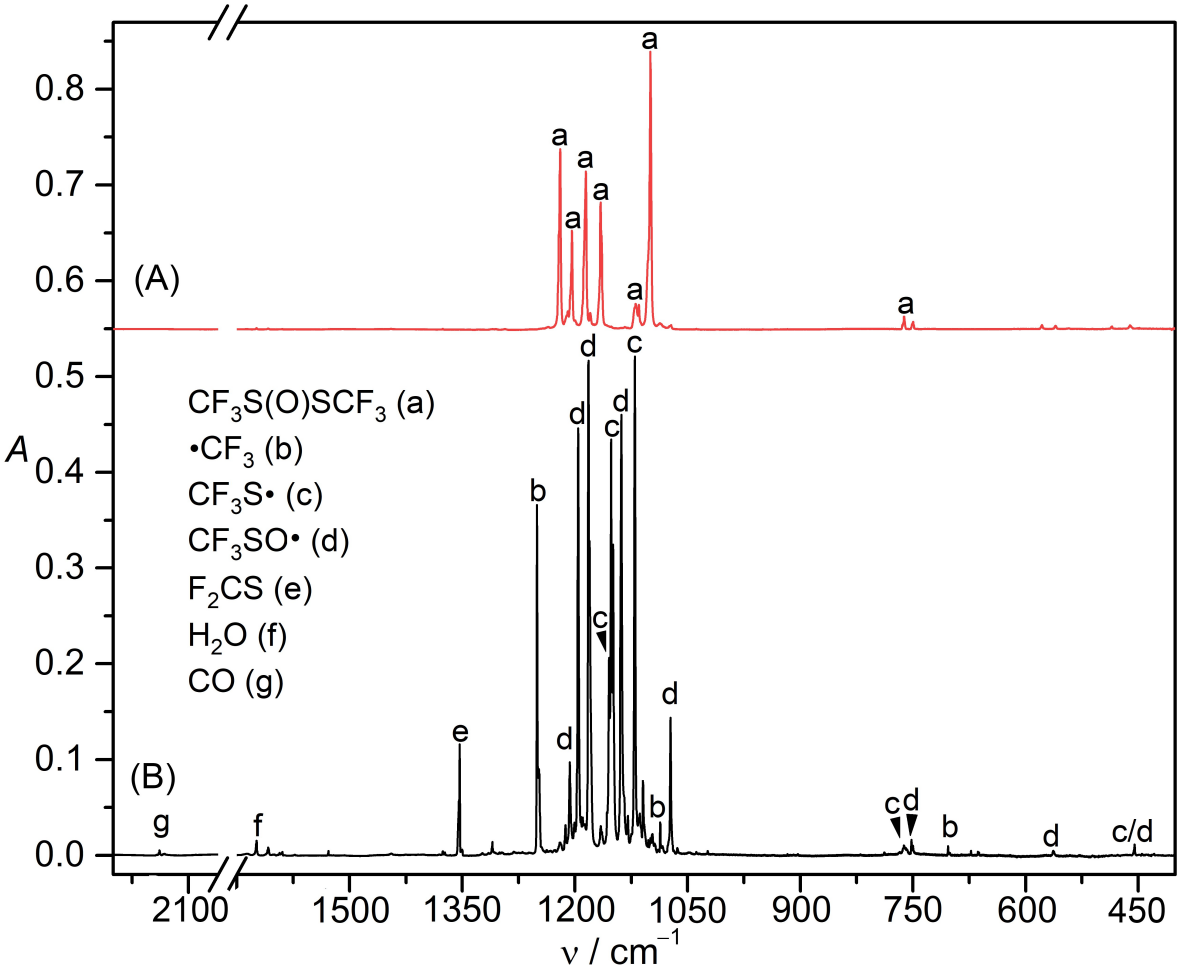

Figure S1. (A) IR spectrum of a 1:1000 mixture of $CF_3S(O)SCF_3$/Ar at 10 K. (B) IR spectrum of the matrix-isolated high-vacuum flash pyrolysis (HVFP, 400 °C) products of a 1:1000 mixture of $CF_3S(O)SCF_3$/Ar at 10 K.

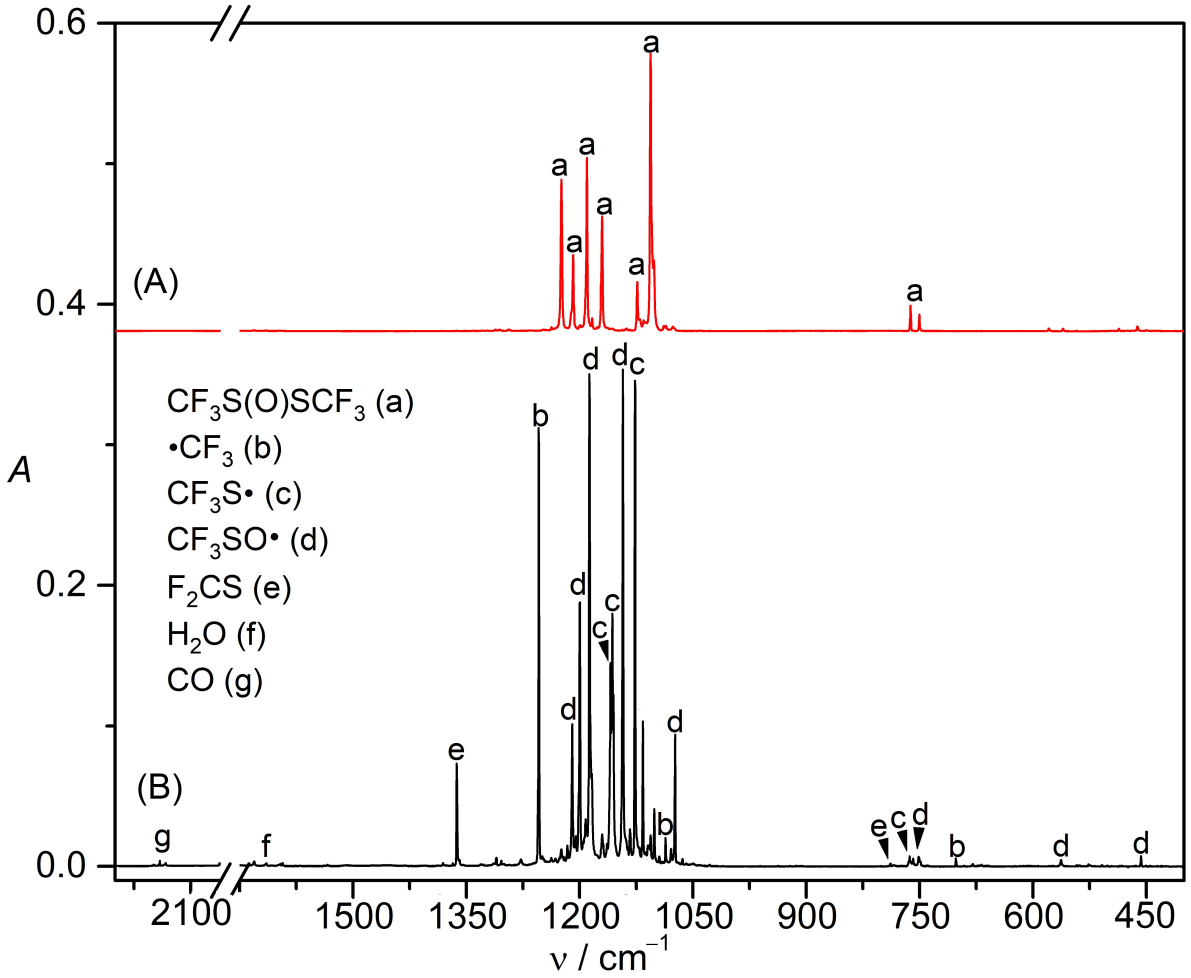

Figure S2. (A) IR spectrum of a 1:1000 mixture of $CF_3S(O)SCF_3$/Ne at 3 K. (B) IR spectrum of the matrix-isolated high-vacuum flash pyrolysis (HVFP, 400 °C) products of a 1:1000 mixture of $CF_3S(O)SCF_3$/Ne at 3 K.

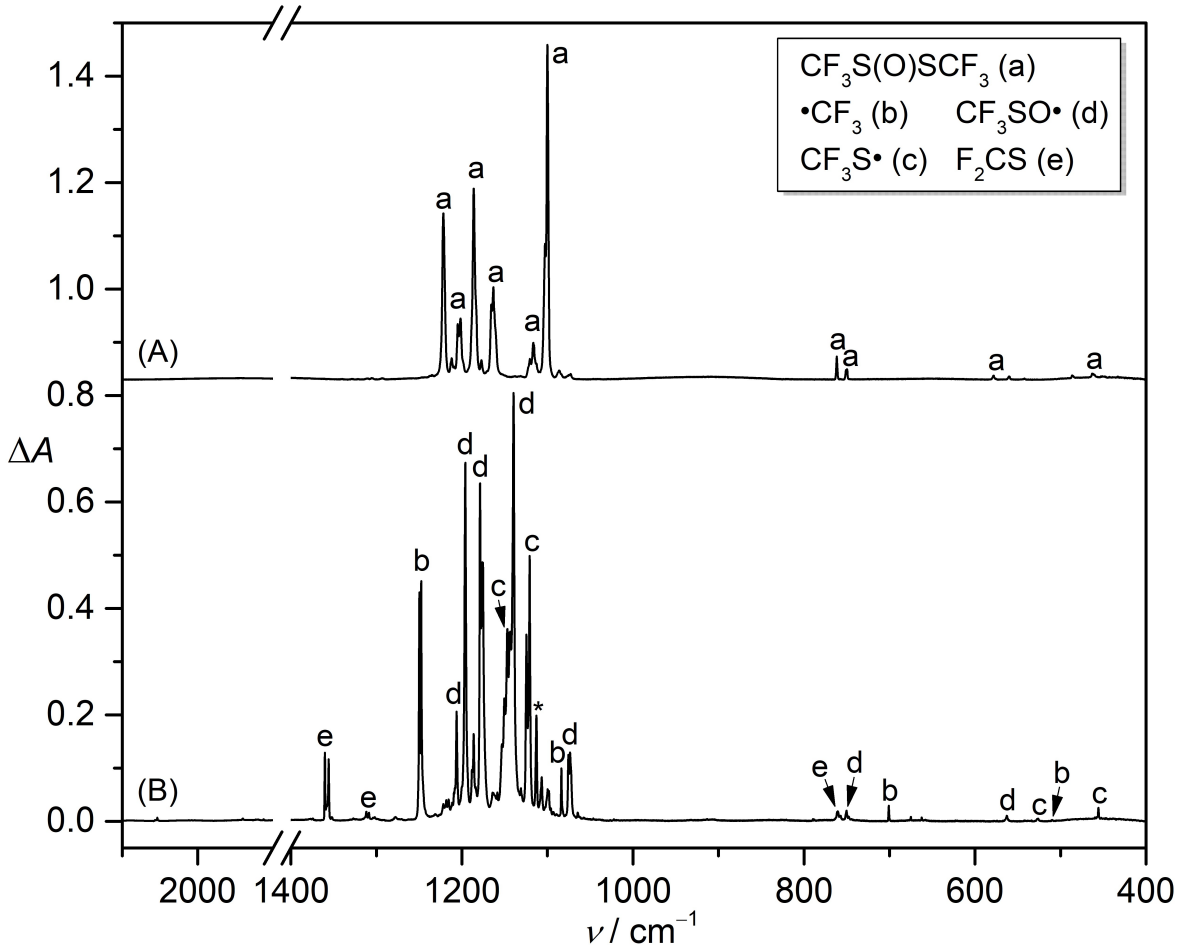

Figure S3. (A) IR spectrum of a 1:1000 mixture of $CF_3S(O)SCF_3/N_2$ at 10 K. (B) IR spectrum of the matrix-isolated high-vacuum flash pyrolysis (HVFP, 400 °C) products of a 1:1000 mixture of $CF_3S(O)SCF_3/N_2$ at 10 K.

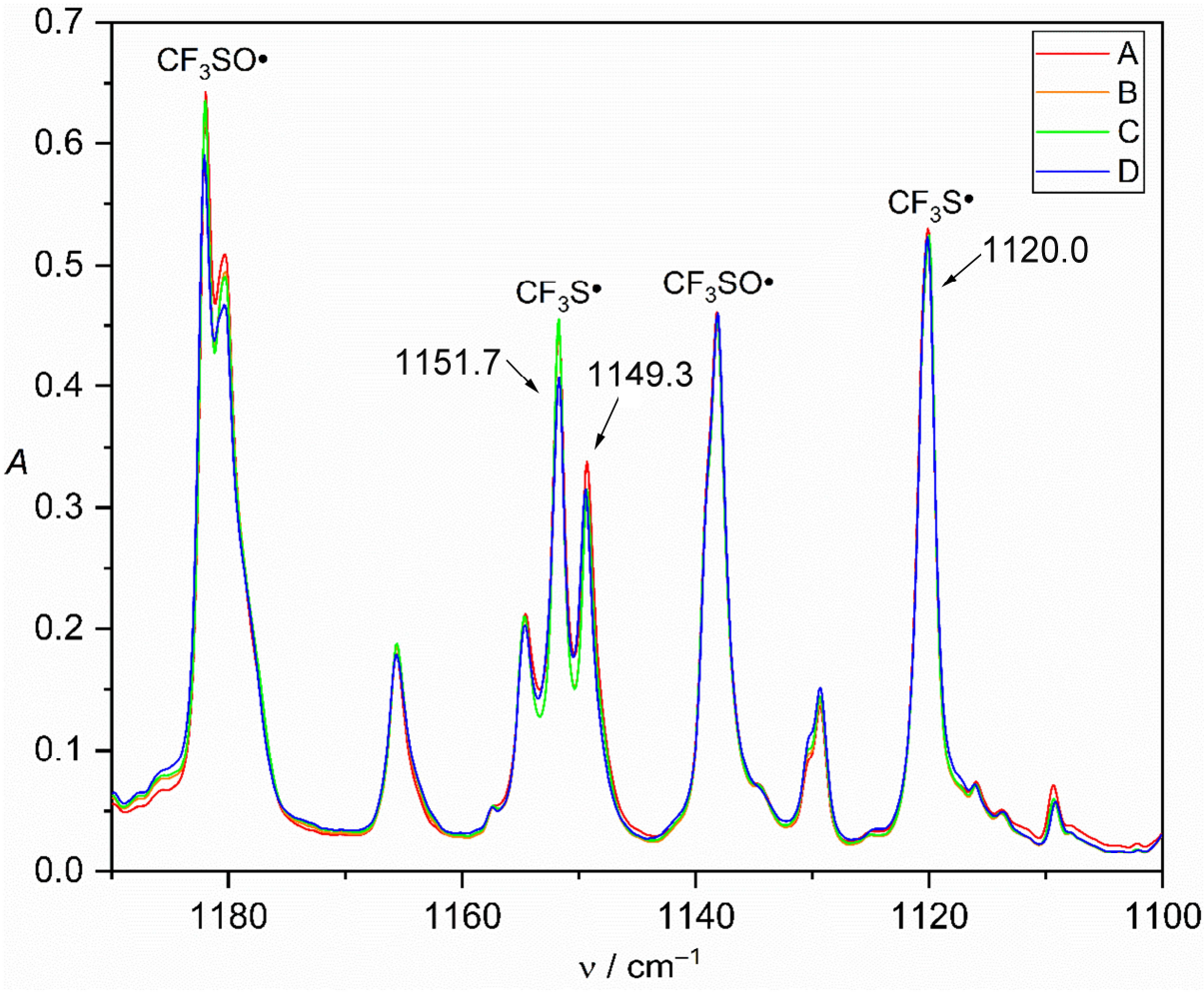

Figure S4. IR spectra in the region of 1190–1100 cm^{-1} obtained: A) 1 h of sample deposition of high-vacuum flash pyrolysis products of $CF_3S(O)SCF_3$/Ar at 10 K, B) after annealing the matrix to 25 K for 1 min, C) after annealing the matrix to 25 K for 5 min, D) after keeping the matrix at 25 K.

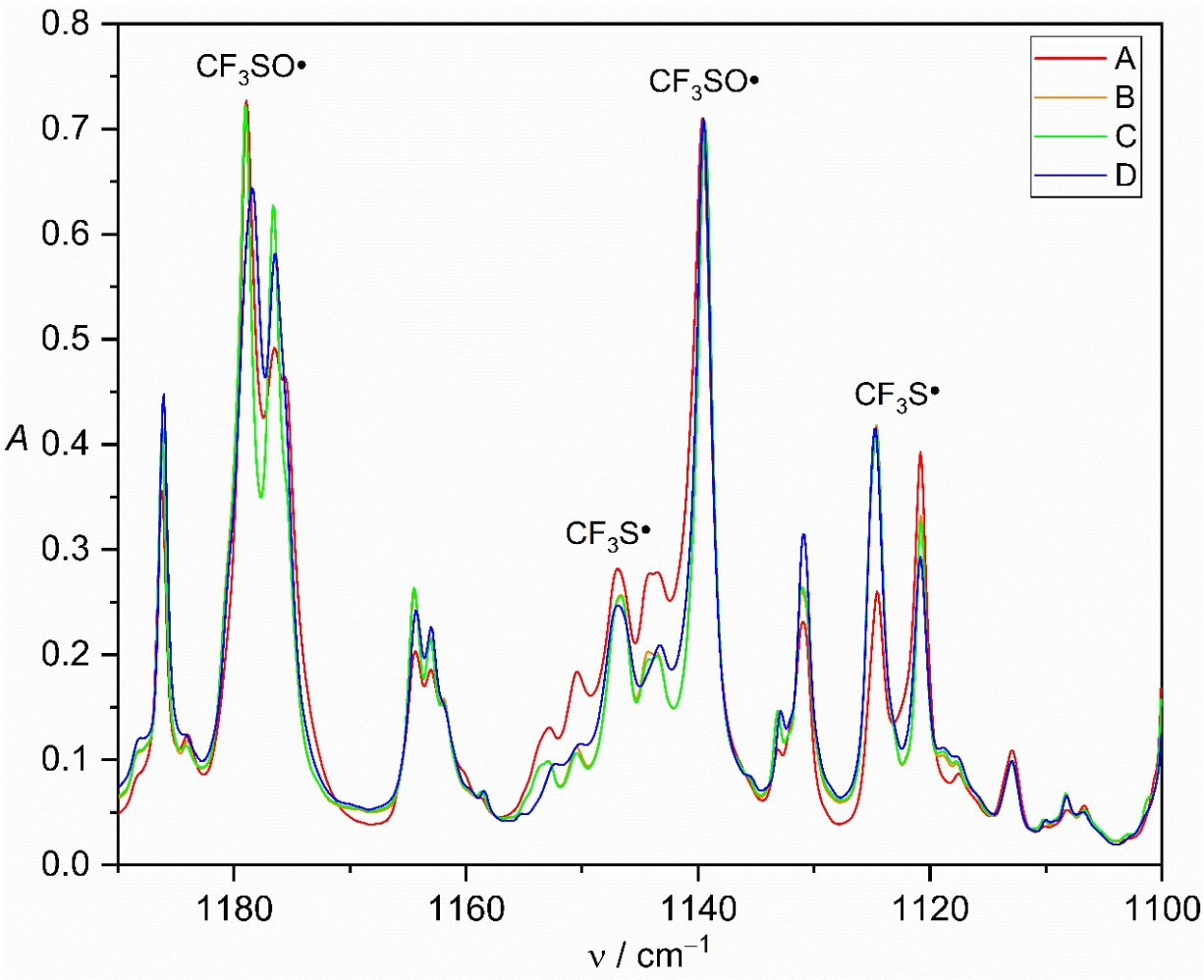

Figure S5. IR spectra in the region of 1190–1100 cm^{-1} obtained: A) 1 h of sample deposition of high-vacuum flash pyrolysis products of $CF_3S(O)SCF_3/N_2$ at 10 K, B) after annealing the matrix to 25 K for 30 s, C) after annealing the matrix to 25 K for 5 min, D) after keeping the matrix at 25 K.

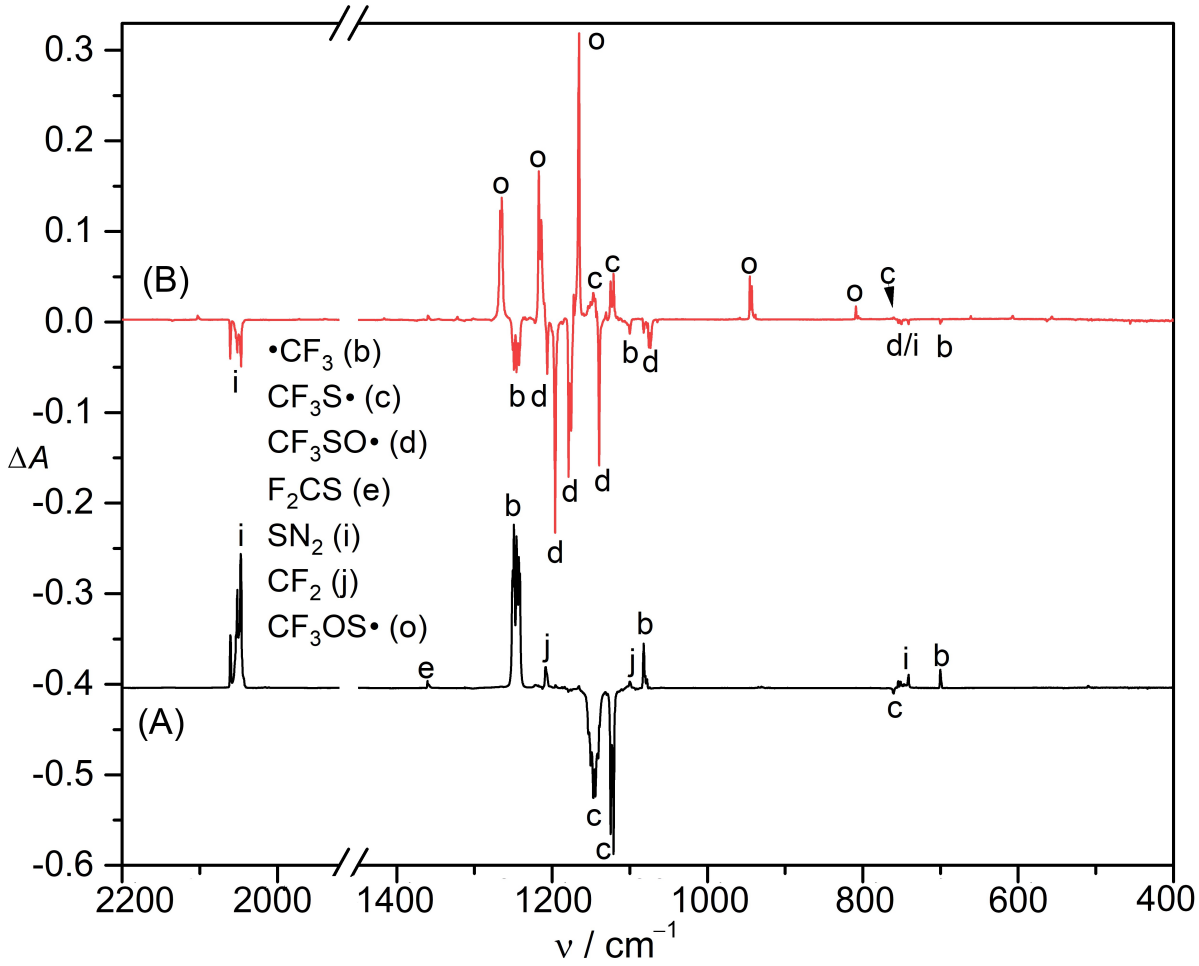

Figure S6. (A) IR difference spectrum showing the changes of the HVFP products of a 1:1000 mixture of $CF_3S(O)SCF_3/N_2$ upon UV-light irradiation (365 nm, 40 min) in a solid N_2-matrix at 10 K. (B) IR difference spectrum showing the changes of the matrix upon further UV-laser irradiation (266 nm, 15 min) at 10 K.

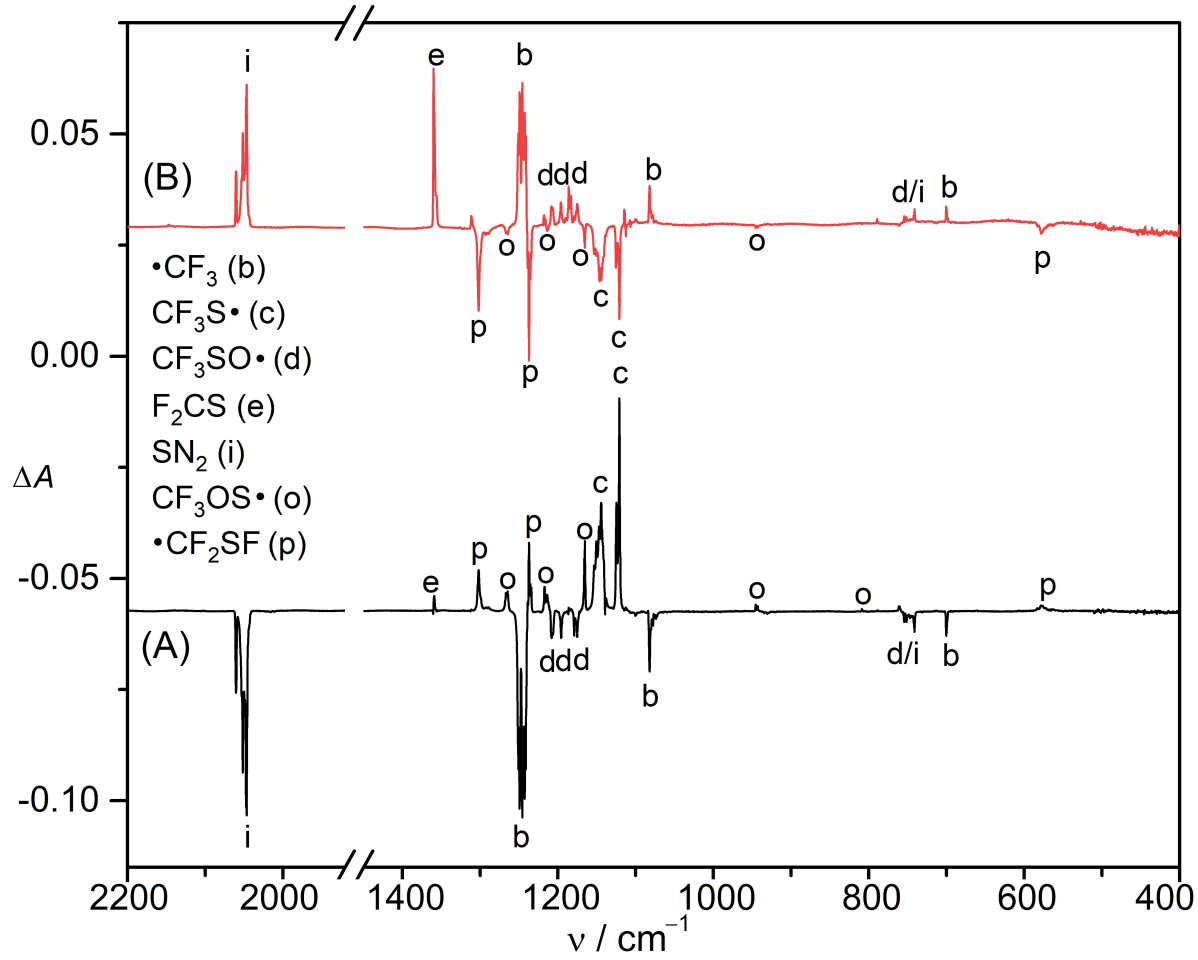

Figure S7. (A) IR difference spectrum showing the changes of the HVFP products of a 1:1000 mixture of $CF_3S(O)SCF_3/N_2$ upon an ArF excimer laser irradiation (193 nm, 30 min) in a solid N_2-matrix at 10 K. (B) IR difference spectrum showing the changes of the matrix upon further UV-light irradiation (365 nm, 5 min) at 10 K.

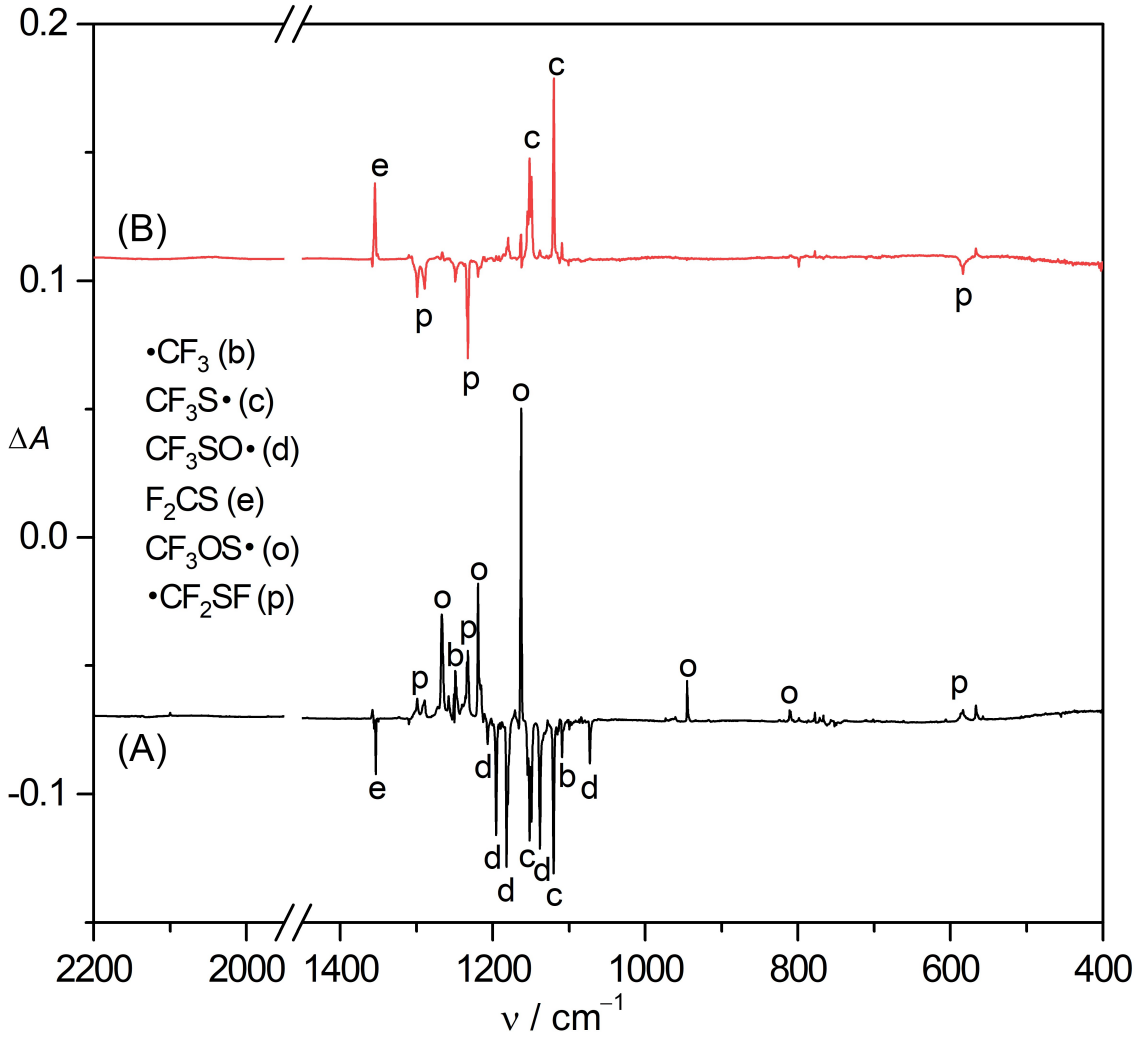

Figure S8. (A) IR difference spectrum showing the changes of the HVFP products of a 1:1000 mixture of $CF_3S(O)SCF_3$/Ar upon an ArF excimer laser irradiation (193 nm, 35 min) in a solid Ar-matrix at 10 K. (B) IR difference spectrum showing the changes of the matrix upon further UV-light irradiation (365 nm, 10 min) at 10 K.

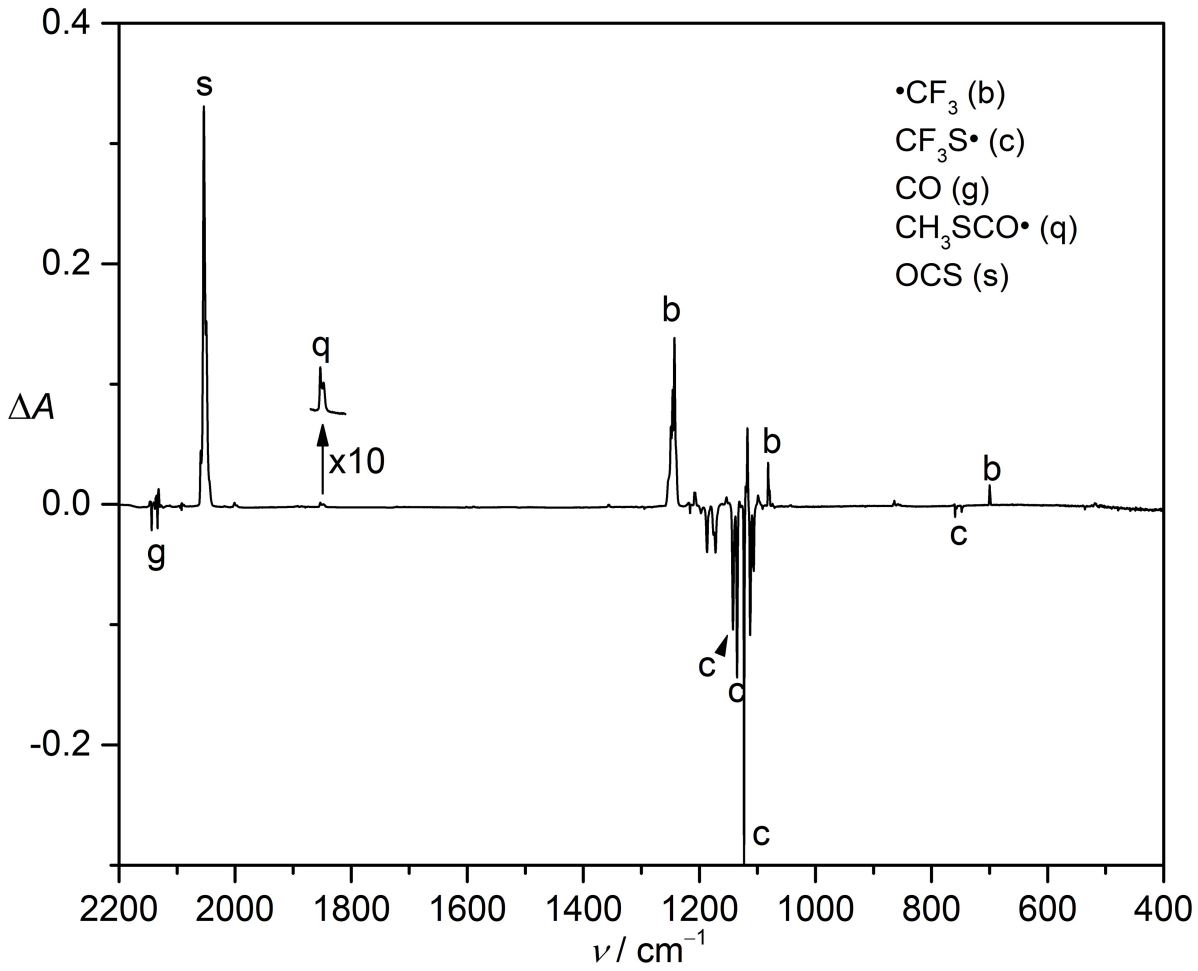

Figure S9. IR difference spectrum showing the changes of the HVFP products of a 1:600 mixture of $CF_3S(O)SCF_3$/CO upon UV-light irradiation (365 nm, 5 min) at 16 K.

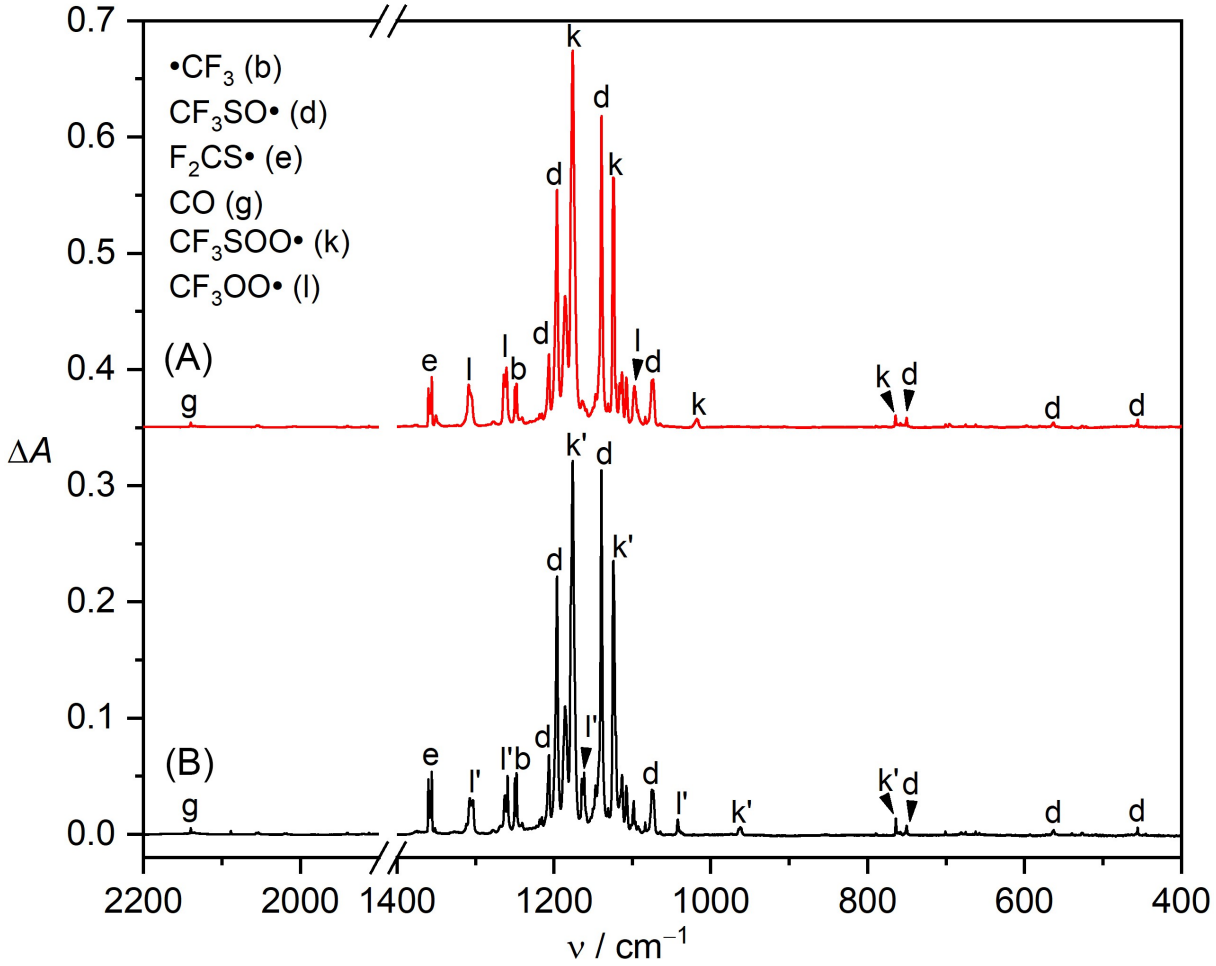

Figure S10. (A) IR spectrum of the HVFP products of a 1:50:1000 mixture of $CF_3S(O)SCF_3/O_2/N_2$ at 10 K. (B) IR spectrum of the HVFP products of a 1:25:25:1000 mixture of $CF_3S(O)SCF_3/O_2/^{18}O_2/N_2$ at 10 K.

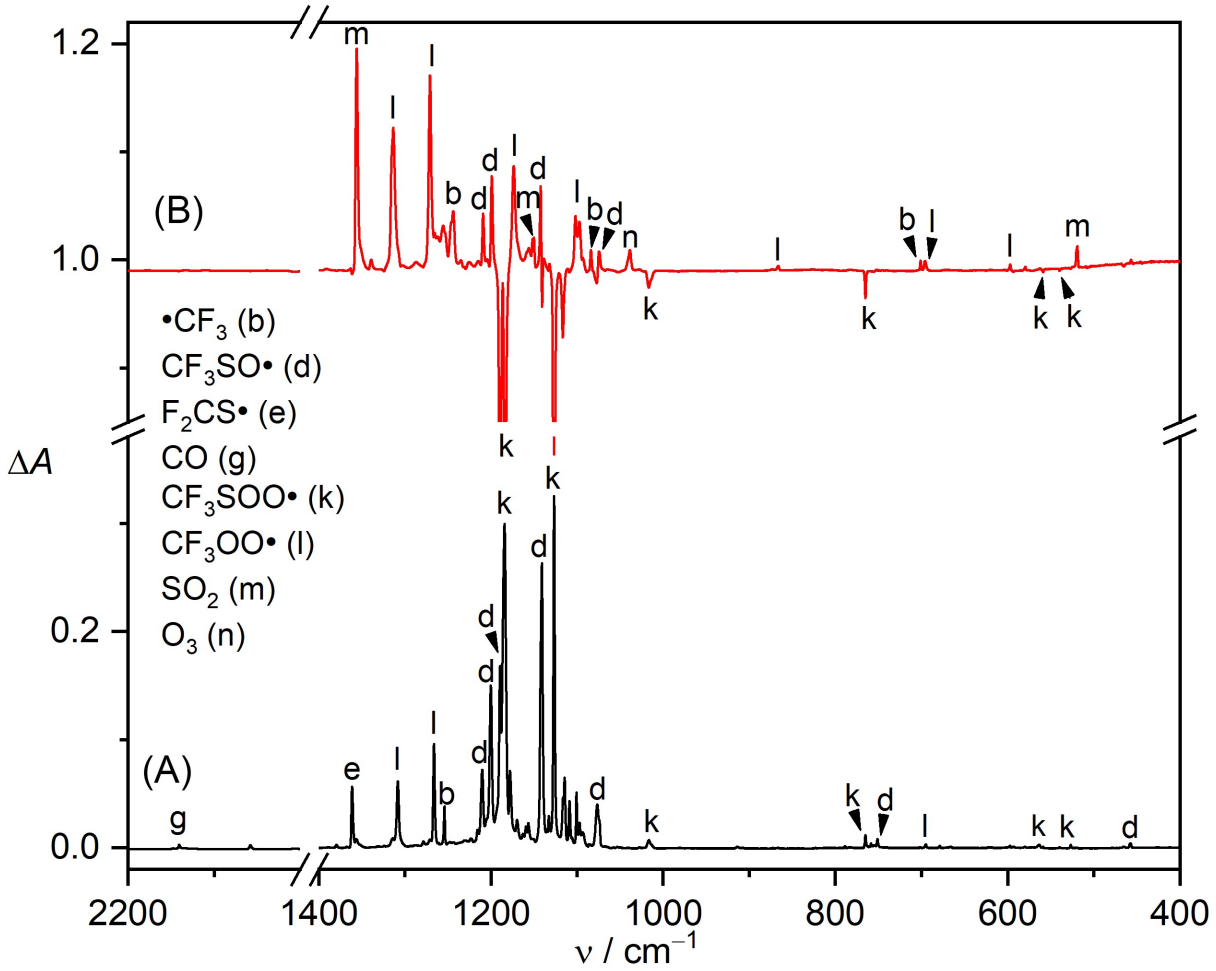

Figure S11. (A) IR spectrum of the HVFP products of a 1:50:1000 mixture of $CF_3S(O)SCF_3/O_2/Ne$ at 3 K. (B) IR difference spectrum showing the change of the matrix upon blue-light LED irradiation (440 nm, 70 min) at 3 K.

Table S1. Calculated IR frequencies (cm^{-1}) and intensity (km mol^{-1}, in parentheses) of $CF_3SSO•$ and its isomers at the MPW1PW91 and B3LYP methods using 6-311+G(3df) basis set.

$CF_3SSO•$		$CF_3SOS•$		$CF_3S(O)S•$		$CF_3OSS•$	
B3LYP	MPW1PW91	B3LYP	MPW1PW91	B3LYP	MPW1PW91	B3LYP	MPW1PW91
1160.5 (222)	1207.9 (218)	1161.3 (220)	1208.6 (222)	1220.7 (283)	1265.9 (285)	1225.1 (486)	1270.9 (446)
1148.0 (234)	1196.1 (232)	1150.6 (238)	1195.9 (240)	1207.8 (253)	1250.9 (254)	1168.9 (610)	1210.2 (341)
1106.6 (92)	1138.0 (101)	1104.0 (417)	1138.9 (407)	1155.9 (43)	1198.3 (48)	1157.6 (342)	1205.3 (629)
1074.0 (423)	1106.4 (416)	759.0 (14)	798.5 (46)	1063.9 (411)	1101.3 (400)	912.1 (32)	940.5 (42)
753.9 (23)	774.0 (26)	756.2 (30)	779.5 (14)	743.4(27)	766.0 (23)	705.8 (57)	738.4 (75)
550.7 (1)	562.5 (2)	610.4 (9)	658.1 (11)	572.6 (20)	612.1 (26)	650.8 (52)	676.9 (41)
536.4 (0.7)	547.3 (1)	551.3 (1)	564.6 (1)	540.8 (1)	555.7 (0.8)	646.8 (1)	660.9 (2)
442.7 (26)	471.4 (41)	532.7 (0.8)	543.4 (1)	537.2 (1)	548.8 (2)	609.9 (1)	623.1 (2)
436.9 (18)	452.4 (4)	460.3 (8)	474.2 (9)	405.2 (12)	423.5 (14)	510.7 (49)	532.0 (43)
350.0 (4)	358.9 (4)	363.5 (0.8)	372.3 (0.8)	362.6 (2)	372.9 (2)	440.4 (0.9)	450.3 (0.9)
312.6 (3)	318.7 (2)	317.3 (0.4)	324.8 (0.4)	310.4 (0.2)	321.0 (0.2)	371.2 (42)	386.7 (30)
253.4 (0.9)	263.9 (0.6)	259.3 (0.3)	263.0 (0.2)	254.5 (2)	265.1 (2)	231.5 (4)	241.9 (3)
126.1 (0.6)	128.4 (0.6)	171.9 (2)	175.9 (2)	194.0 (3)	197.3 (3)	181.7 (1)	184.8 (1)
57.7 (2)	58.2 (2)	52.4 (< 0.1)	53.2 (< 0.1)	139.7 (0.2)	142.9 (0.2)	58.4 (< 0.1)	60.6 (< 0.1)
35.8 (0.7)	35.1 (0.7)	41.2 (< 0.1)	48.6 (< 0.1)	46.5 (0.3)	48.1 (0.3)	32.3 (0.1)	33.9 (0.1)

Table S2. Calculated IR frequencies (cm^{-1}) and intensity (km mol^{-1}, in parentheses) of $CF_3S\bullet$ at the MPW1PW91, B3LYP and BP86 methods using 6-311+G(3df) basis set.

$CF_3S\bullet$			$\bullet CF_2SF$		
MPW1PW91	B3LYP	BP86	MPW1PW91	B3LYP	BP86
1181.2 (255)	1134.1 (253)	1071.9 (243)	1339.9 (300)	1304.4 (314)	1271.1 (326)
1172.0 (282)	1123.7 (284)	1055.9 (329)	1278.6 (246)	1232.9 (244)	1173.6 (232)
1136.4 (370)	1102.5 (359)	1040.4 (276)	734.9 (4)	721.3 (4)	714.9 (7)
778.5 (11)	758.2 (10)	727.9 (8)	592.8 (159)	522.3 (155)	478.9 (88)
545.3 (2)	535.0 (1)	512.4 (1)	500.0 (16)	489.8 (13)	466.8 (58)
543.8 (0.5)	532.6 (0.3)	509.2 (< 0.1)	392.2 (4)	391.7 (8)	413.1 (13)
459.1 (3)	445.8 (3)	431.8 (2)	373.9 (0.3)	367.1 (0.2)	353.4 (1)
293.3 (0.3)	288.8 (0.3)	270.4 (0.3)	183.1 (3)	177.6 (3)	157.7 (2)
207.9 (0.5)	201.7 (0.6)	198.4 (0.7)	105.0 (1)	115.8 (1)	131.8 (2)

Table S3. Calculated vertical transitions (nm) for $CF_3S\bullet$.

EOM[a]	CASSCF[b]	MRCI+Q	TD-B3LYP[c]
19410 (0)	17854.0	22960	11092.1 (0)
322.4 (0.0029)	287.3	324.9	370.9 (0.0006)
211.3 (0)	164.7	178.3	236.8 (0.0006)
181.2 (0.0012)			225.5 (0)
			212.7 (0.0001)
			209.6 (0.0094)
			193.9 (0.0001)

[a] At the EOM-CCSD/aug-cc-pV(T+d)Z level of theory. The oscillator strengths are given in parentheses. [b] The CASSCF/aug-cc-pv(T+d)z active space is (21,15) and all CI configurations with weight greater than 0.01 were considered. Calculation were done in C_s symmetry at the optimized equilibrium geometry at CCSD(T)/aug-cc-pv(T+d)z. [c] At the 6-311+G(3df) basis set.

Table 4. Computed and observed IR data for $\bullet CF_2SF$.

ν_{cal}[a]	ν_{obs}[b]		Mode[c]
CCSD(T)	N_2-matrix	Ar-matrix	$\bullet CF_2SF$
1315.3	1301.9	1299.1	ν_1, $\nu_s(CF_2)$
1265.5	1237.2	1232.6	ν_2, $\nu_{as}(CF_2)$
712.4	713.2	710.7	ν_3, ν(CS)
623.3	578.1	583.4	ν_4, ν(SF)
494.4	491.4	490.3	ν_5, $\delta(CF_2)$

[a] Harmonic IR frequencies calculated harmonic frequencies at the aug-cc-pV(T+d)Z basis set. [b] Observed band positions for the most intense matrix sites. [c] Tentative assignment of the vibration modes based on the computed vibrational displacement vectors for $\bullet CF_2SF$.

Table S5. Computed and observed IR data for $CF_3SOO•$.

ν_{cal}[a]	ν_{obs}[b]		$\Delta\nu(O/^{18}O)$[c]		Mode[d]
CCSD(T)	N_2-matrix	Ne-matrix	obs	cal	
1172.9	1185.1	1189.5	< 0.5	0.2	ν_1, $\nu_{as}(CF_3)$
1169.2	1176.1	1183.8	< 0.5	–0.1	ν_2, $\nu_{as}(CF_3)$
1118.9	1124.1	1126.9	< 0.5	0.4	ν_3, $\nu_s(CF_3)$
1013.7	1017.6	1016.6	55.5	56.2	ν_4, ν(OO)
741.0	764.4	765.1	0.5	–0.1	ν_5, $\delta(CF_3)$
584.4	558.6	559.0	18.8	28.6	ν_6, ν(SO)
539.6	n.o.[e]	n.o.[e]	n.o.	0.1	ν_7, $\delta(CF_3)$
520.2	540.0	539.7	< 0.5	0.3	ν_8, $\delta(CF_3)$
461.0	463.3	465.1	< 0.5	5.6	ν_9, ν(CS)

[a] Harmonic IR frequencies (> 400 cm^{-1}) calculated at the aug-cc-pV(D+d)Z basis set. Full list of the calculated IR frequencies is given in Table S7. [b] Observed band positions for the most intense matrix sites. [c] Observed and calculated ^{18}O-isotopic shifts. [d] Tentative assignment of the vibration modes based on the computed vibrational displacement vectors. [e] Not observed due to low intensity.

Table S6. Calculated vertical transitions (nm) for $CF_3SOO•$.

EOM[a]	CASSCF[b]	TD-B3LYP[c]
1211 (0)	1227	1045.2 (0)
354.4 (0)	398.6	437.3 (0.0005)
302.7 (0.0022)	386.2	392.1 (0)
295.8 (0.0003)		342.2 (0.0012)
		303.5 (0.0006)
		283.8 (0.0006)
		252.9 (0.0170)
		229.3 (0.1240)
		217.4 (0.0001)
		207.4 (0.0006)

[a] At the EOM-CCSD/aug-cc-pV(T+d)Z level of theory. The oscillator strengths are given in parentheses. [b] CASSCF/aug-cc-pv(D+d)Z with an active space (15,14). [c] At the 6-311+G(3df) basis set.

Table S7. Calculated IR frequencies (cm^{-1}) and intensity (km mol^{-1}, in parentheses) of $CF_3SOO•$, $CF_3OSO•$ and CF_3SO_2 at the MPW1PW91, B3LYP and BP86 methods using 6-311+G(3df) basis set.

$CF_3SOO•$			$CF_3OSO•$			$CF_3SO_2•$		
MPW1PW91	B3LYP	BP86	MPW1PW91	B3LYP	BP86	MPW1PW91	B3LYP	BP86
1210.8 (217)	1164.6 (219)	1279.9 (226)	1281.7 (402)	1236.2 (408)	1172.3 (371)	1350.9 (221)	1301.3 (217)	1239.8 (208)
1207.0 (255)	1162.0 (256)	1093.6 (237)	1243.7 (226)	1206.5 (183)	1158.2 (121)	1267.7 (157)	1224.4 (263)	1168.9 (277)
1156.8 (58)	1116.0 (117)	1074.1 (118)	1217.5 (242)	1170.6 (264)	1109.7 (267)	1267.7 (283)	1223.4 (177)	1168.3 (149)
1129.9 (358)	1090.6 (307)	1028.5 (404)	1175.2 (526)	1136.9 (547)	1081.6 (587)	1144.3 (19)	1101.7 (12)	1046.6 (15)
780.3 (14)	760.3 (14)	730.3 (15)	948.7 (76)	919.7 (67)	872.1 (54)	1081.4 (352)	1043.8 (371)	989.6 (351)
623.0 (4)	579.0 (8)	563.5 (18)	761.1 (91)	729.1 (88)	685.4 (88)	758.3 (28)	734.7 (33)	701.6 (36)
565.1 (0.9)	552.8 (0.5)	512.7 (0.3)	659.9 (1)	646.2 (0.5)	617.4 (0.4)	564.4 (2)	551.1 (1)	524.9 (0.5)
544.6 (1)	534.1 (0.9)	511.5 (7)	626.5 (5)	613.4 (4)	584.1 (2)	551.7 (1)	539.5 (0.8)	515.3 (0.4)
469.0 (8)	454.6 (7)	403.3 (10)	544.8 (43)	527.3 (48)	503.6 (50)	499.2 (38)	487.8 (36)	459.3 (29)
421.0 (0.1)	390.3 (0.6)	335.8 (15)	473.3 (7)	462.0 (7)	437.1 (6)	450.2 (20)	431.9 (19)	402.7 (14)
325.1 (0.4)	317.0 (0.5)	300.5 (0.1)	406.4 (19)	397.6 (24)	378.5 (22)	334.9 (0.3)	322.7 (0.2)	300.6 (0.2)
297.3 (0.2)	284.7 (0.7)	202.4 (16)	315.1 (2)	304.0 (3)	286.6 (4)	276.9 (1)	256.5 (1)	232.8 (1)
172.8 (1)	166.2 (0.9)	115.2 (0.2)	178.4 (1)	175.9 (1)	165.0 (1)	203.7 (5)	198.1 (4)	181.4 (3)
69.4 (0.4)	60.3 (0.4)	66.2 (< 0.1)	73.3 (1)	69.3 (1)	60.9 (0.8)	171.9 (1)	168.8 (1)	154.8 (1)
52.2 (0.3)	50.8 (0.4)	30.6 (< 0.1)	37.7 (3)	36.1 (3)	32.1 (3)	50.2 (0.3)	47.4 (0.3)	42.9 (0.3)

Table S8. Calculated vertical transitions (nm) for $\bullet CF_2SF$.

EOM[a]	CASSCF[b]	MRCI+Q	TD-B3LYP[c]
526.4 (0.0011)	612	641.0	592.8 (0.0015)
278.5 (0.0212)	264	281.7	316.3 (0.0219)
241.7 (0.0090)			271.4 (0.0018)
238.0 (0.0075)			267.6 (0.0036)
			227.7 (0.0047)
			210.3 (0.0337)
			202.1 (0.0173)
			198.3 (0.0101)
			194.0 (0.0142)
			190.5 (0.0302)

[a] At the EOM-CCSD/aug-cc-pV(T+d)Z level of theory. The oscillator strengths are given in parentheses. [b] The CASSCF/aug-cc-pv(T+d)z active space is (15,13) and all CI configurations with weight greater than 0.02 were considered. Calculation were done in C_1 symmetry using at the optimized equilibrium geometry at CCSD(T)/aug-cc-pv(T+d)z. [c] At the 6-311+G(3df) basis set.

Calculated atomic coordinates (in Angstroms) and energies (in Hartrees) for all optimized structures.

CF_3S•

B3LYP/6-311+G(3df)

C	-0.32581400	-0.02808700	0.00000000
F	-0.80668100	1.22351300	0.00000000
F	-0.80668100	-0.66249000	1.07580600
F	-0.80668100	-0.66249000	-1.07580600
S	1.48345400	0.06760700	0.00000000

Zero-point correction= 0.013949
Thermal correction to Energy= 0.018602
Thermal correction to Enthalpy= 0.019546
Thermal correction to Gibbs Free Energy= -0.015216
Sum of electronic and zero-point Energies= -735.921357
Sum of electronic and thermal Energies= -735.916704
Sum of electronic and thermal Enthalpies= -735.915760
Sum of electronic and thermal Free Energies= -735.950522

UCCSD(T)/aug-cc-pV(T+d)Z

S	0.00000000	0.00000000	0.00000000
C	0.00000000	0.00000000	1.81524773
F	1.27109873	0.00000000	2.23185027
F	-0.60578518	1.07848777	2.32241142
F	-0.60778568	-1.06652598	2.31740908

•CF_2SF

B3LYP/6-311+G(3df)

F	-1.63407600	-0.77431900	0.47265300
C	-0.72133800	-0.02388600	-0.11150100
F	-1.16084200	1.20618300	-0.24054800
S	0.82815300	-0.50378300	-0.41755100
F	1.80353800	0.47967400	0.58454100

Zero-point correction= 0.012127
Thermal correction to Energy= 0.017491
Thermal correction to Enthalpy= 0.018436
Thermal correction to Gibbs Free Energy= -0.018007
Sum of electronic and zero-point Energies= -735.879753
Sum of electronic and thermal Energies= -735.874389
Sum of electronic and thermal Enthalpies= -735.873445
Sum of electronic and thermal Free Energies= -735.909888

UCCSD(T)/aug-cc-pV(T+d)Z ENERGY=-734.91431399

C	-0.0429281150	-0.1561965337	-0.7198102422
S	-0.4485182969	-0.4756541275	0.8669300206
F	0.4208327208	0.6392234865	1.7537904493
F	1.1888871911	-0.2068719214	-1.1822474243
F	-0.8257010557	0.4690688276	-1.5794243528

***cis*-CF_3SOO•**

B3LYP/6-311+G(3df)

C	0.91428100	0.12648600	-0.00471000
S	-0.46963000	-1.06330800	-0.10939700

F 1.99452400 -0.53012600 -0.44624400
F 0.72465800 1.20473600 -0.76204100
F 1.14214900 0.54210300 1.24027200
O -1.69922100 0.01534100 0.54185300
O -2.39122500 0.64760900 -0.35551000
Zero-point correction= 0.019784
Thermal correction to Energy= 0.027034
Thermal correction to Enthalpy= 0.027978
Thermal correction to Gibbs Free Energy= -0.013981
Sum of electronic and zero-point Energies= -886.301457
Sum of electronic and thermal Energies= -886.294206
Sum of electronic and thermal Enthalpies= -886.293262
Sum of electronic and thermal Free Energies= -886.335222

UCCSD(T)/aug-cc-pV(D+d)Z ENERGY=-884.66375315
S 0.1328123766 -1.1154751219 -0.4765464492
C 0.0023292982 0.1154543298 0.8569533791
O -0.5549494095 -0.0311232565 -1.7183814540
F 0.4547185389 -0.4861732350 1.9847971132
F -1.2669867673 0.5239284347 1.0645022702
F 0.7463763539 1.2160626207 0.6247773523
O 0.3653109474 0.6908276336 -2.3327941121

***trans*-$CF_3SOO\bullet$**
B3LYP/6-311+G(3df)
C 1.00054400 -0.08531200 0.00007400
S -0.52902100 0.91122900 -0.00018800
F 2.00965800 0.79413800 0.00037500
F 1.10649500 -0.86339700 1.07542400
F 1.10694400 -0.86320100 -1.07537600
O -1.59797500 -0.51006100 -0.00085100
O -2.84537500 -0.19939400 0.00069500
Zero-point correction= 0.019656
Thermal correction to Energy= 0.027127
Thermal correction to Enthalpy= 0.028071
Thermal correction to Gibbs Free Energy= -0.015684
Sum of electronic and zero-point Energies= -886.300701
Sum of electronic and thermal Energies= -886.293230
Sum of electronic and thermal Enthalpies= -886.292286
Sum of electronic and thermal Free Energies= -886.336041

$CF_3OSO\bullet$
B3LYP/6-311+G(3df)
C -1.02415300 -0.03570100 -0.01897700
F -2.04660700 -0.15836100 -0.85368500
F -0.86119300 -1.18516300 0.64055500
F -1.31903200 0.90984500 0.88467600
O 2.29078400 -0.77842800 -0.01087000
O 0.07941800 0.29760600 -0.75453600
S 1.57654900 0.49774300 0.01207500
Zero-point correction= 0.021942
Thermal correction to Energy= 0.028730

Thermal correction to Enthalpy= 0.029674
Thermal correction to Gibbs Free Energy= -0.011648
Sum of electronic and zero-point Energies= -886.436063
Sum of electronic and thermal Energies= -886.429275
Sum of electronic and thermal Enthalpies= -886.428331
Sum of electronic and thermal Free Energies= -886.469653

CF_3SO_2•

B3LYP/6-311+G(3df)

C	0.88755500	-0.00004200	-0.00746700
O	-1.50034900	-1.27138000	-0.19502400
F	1.40285000	1.08456800	0.54296500
F	1.40338700	-1.08278500	0.54536400
F	1.10767700	-0.00142200	-1.30968700
S	-1.03369400	0.00001100	0.32247500
O	-1.50108200	1.27098400	-0.19529800

Zero-point correction= 0.021947
Thermal correction to Energy= 0.028759
Thermal correction to Enthalpy= 0.029704
Thermal correction to Gibbs Free Energy= -0.010863
Sum of electronic and zero-point Energies= -886.397604
Sum of electronic and thermal Energies= -886.390791
Sum of electronic and thermal Enthalpies= -886.389847
Sum of electronic and thermal Free Energies= -886.430413

CF_3SSO•

B3LYP/6-311+G(3df)

C	1.21024900	0.15000600	0.00657600
F	0.99818100	1.27294400	-0.68026200
F	1.32557400	0.48219200	1.29644800
F	2.36906200	-0.38124000	-0.39569000
S	-0.09279900	-1.11381900	-0.28042700
S	-1.79414900	-0.08158300	0.46042400
O	-2.41320800	0.73266900	-0.61298500

Zero-point correction= 0.019014
Thermal correction to Energy= 0.026581
Thermal correction to Enthalpy= 0.027525
Thermal correction to Gibbs Free Energy= -0.015918
Sum of electronic and zero-point Energies= -1209.406697
Sum of electronic and thermal Energies= -1209.399129
Sum of electronic and thermal Enthalpies= -1209.398185
Sum of electronic and thermal Free Energies= -1209.441628

CF_3SOS•

B3LYP/6-311+G(3df)

C	1.23770100	-0.17858100	-0.00905800
F	2.33809100	0.28677600	-0.61486600
F	0.87366200	-1.32251000	-0.59374200
F	1.53135500	-0.45775700	1.26075500
S	-0.01743300	1.13336900	-0.17963500
O	-1.27508600	0.34790800	0.65928500

S -2.47716000 -0.40026600 -0.17594300
Zero-point correction= 0.018891
Thermal correction to Energy= 0.026278
Thermal correction to Enthalpy= 0.027222
Thermal correction to Gibbs Free Energy= -0.015747
Sum of electronic and zero-point Energies= -1209.352900
Sum of electronic and thermal Energies= -1209.345512
Sum of electronic and thermal Enthalpies= -1209.344568
Sum of electronic and thermal Free Energies= -1209.387537

$CF_3S(O)S•$
B3LYP/6-311+G(3df)
C -1.07648000 -0.22174400 0.01210800
F -1.21913200 -0.41574700 1.31307800
F -1.18167600 -1.37282900 -0.63216800
S 0.63268400 0.56802300 -0.37388100
O 0.59151200 1.88882500 0.26056900
S 1.95452800 -0.77106100 0.08980300
F -2.00681600 0.61840600 -0.41557000
Zero-point correction= 0.019947
Thermal correction to Energy= 0.027139
Thermal correction to Enthalpy= 0.028083
Thermal correction to Gibbs Free Energy= -0.013724
Sum of electronic and zero-point Energies= -1209.373889
Sum of electronic and thermal Energies= -1209.366698
Sum of electronic and thermal Enthalpies= -1209.365753
Sum of electronic and thermal Free Energies= -1209.407560

$CF_3OSS•$
B3LYP/6-311+G(3df)
C 1.34597000 -0.10034300 -0.02158300
F 2.33693500 -0.45234200 -0.83390600
F 1.05227900 -1.14147800 0.76915200
F 1.77956500 0.89093000 0.77389700
S -2.42714200 -0.55504900 0.00008000
O 0.29442400 0.28124700 -0.79238200
S -1.13224700 0.84742900 0.00531200
Zero-point correction= 0.020284
Thermal correction to Energy= 0.027377
Thermal correction to Enthalpy= 0.028321
Thermal correction to Gibbs Free Energy= -0.014279
Sum of electronic and zero-point Energies= -1209.424484
Sum of electronic and thermal Energies= -1209.417392
Sum of electronic and thermal Enthalpies= -1209.416448
Sum of electronic and thermal Free Energies= -1209.459047

References

[1] A. D. Becke, *J. Chem. Phys.* **1993**, *98*, 5648–5652.
[2] A. D. Becke, *Phys. Rev. A* **1988**, *38*, 3098–3100.
[3] C. Adamo, V. Barone, *J. Chem. Phys.* **1998**, *108*, 664.
[4] J. A. Montgomery Jr., M. J. Frisch, J. W. Ochterski, G. A. Petersson, *J. Chem. Phys.* **2000**, *112*, 6532–6542.
[5] a) K. Fukui, *Acc. Chem. Res*. **1981**, *4*, 363−368; b) H. P. Hratchian, H. B. Schlegel, *J. Chem. Theory Comput.* **2005**, *1*, 61−69.
[6] a) R. E. Stratmann, G. E. Scuseria, M. J. Frisch, *J. Chem. Phys.* **1998**, *109*, 8218; b) J. B. Foresman, M. Head-Gordon, J. A. Pople, M. J. Frisch, *J. Phys. Chem.* **1992**, *96*, 135-149.
[7] T. Korona, H.-J. Werner, *J. Chem. Phys.* **2003**, *118*, 3006−3019.
[8] M. J. Frisch, G. W. Trucks, H. B. Schlegel, G. E. Scuseria, M. A. Robb, J. R. Cheeseman, G. Scalmani, V. Barone, B. Mennucci, G. A. Petersson, H. Nakatsuji, M. Caricato, X. Li, H. P. Hratchian, A. F. Izmaylov, J. Bloino, G. Zheng, J. L. Sonnenberg, M. Hada, M. Ehara, K. Toyota, R. Fukuda, J. Hasegawa, M. Ishida, T. Nakajima, Y. Honda, O. Kitao, H. Nakai, T. Vreven, J. A. Montgomery, Jr., J. E. Peralta, F. Ogliaro, M. Bearpark, J. J. Heyd, E. Brothers, K. N. Kudin, V. N. Staroverov, R. Kobayashi, J. Normand, K. Raghavachari, A. Rendell, J. C. Burant, S. S. Iyengar, J. Tomasi, M. Cossi, N. Rega, J. M. Millam, M. Klene, J. E. Knox, J. B. Cross, V. Bakken, C. Adamo, J. Jaramillo, R. Gomperts, R. E. Stratmann, O. Yazyev, A. J. Austin, R. Cammi, C. Pomelli, J. W. Ochterski, R. L. Martin, K. Morokuma, V. G. Zakrzewski, G. A. Voth, P. Salvador, J. J. Dannenberg, S. Dapprich, A. D. Daniels, Ö. Farkas, J. B. Foresman, J. V. Ortiz, J. Cioslowski, and D. J. Fox, Gaussian, Inc., Wallingford CT, Gaussian 09, Revision A.2.
[9] a) P. J. Knowles and H.-J. Werner, *Chem. Phys. Lett.* **1985**, *115*, 259–267; b) H. J. Werner, P. J. Knowles, *J. Chem. Phys.* **1985**, *82*, 5053–5063.
[10] a) H.-J. Werner, P. J. Knowles, *J. Chem. Phys.* **1988**, *89*, 5803–5814; b) P. J. Knowles and H.-J. Werner, *Chem. Phys. Lett.* **1988**, *145*, 514–522.
[11] H.-J. Werner, P. J. Knowles, G. Knizia, F. R. Manby, M. Schütz, *Wiley Interdiscip. Rev.: Comput. Mol. Sci*. **2012**, *2*, 242–253.